



Article

Integrating Soft Hydrogel with Nanostructures Reinforces Stem Cell Adhesion and Differentiation

Bohan Yin ¹, Hongrong Yang ² and Mo Yang ^{1,*}

¹ Department of Biomedical Engineering, The Hong Kong Polytechnic University, Hong Kong 999077, China; bohanyin93@gmail.com

² Department of Bioengineering, College of Engineering, Northeastern University, Boston, MA 02115, USA; donnayeung0722@gmail.com

* Correspondence: mo.yang@polyu.edu.hk; Tel.: +852-2766-4946

Abstract: Biophysical cues can regulate stem cell behaviours and have been considered as critical parameters of synthetic biomaterials for tissue engineering. In particular, hydrogels have been utilized as promising biomimetic and biocompatible materials to emulate the microenvironment. Therefore, well-defined mechanical properties of a hydrogel are important to direct desirable phenotypes of cells. Yet, limited research pays attention to engineering soft hydrogel with improved cell adhesive property, which is crucial for stem cell differentiation. Herein, we introduce silica nanoparticles (SiO₂ NPs) onto the surface of methacrylated hyaluronic (MeHA) hydrogel to manipulate the presentation of cell adhesive ligands (RGD) clusters, while remaining similar bulk mechanical properties (2.79 ± 0.31 kPa) to that of MeHA hydrogel (3.08 ± 0.68 kPa). RGD peptides are either randomly decorated in the MeHA hydrogel network or on the immobilized SiO₂ NPs (forming MeHA–SiO₂). Our results showed that human mesenchymal stem cells exhibited a ~1.3-fold increase in the percentage of initial cell attachment, a ~2-fold increase in cell spreading area, and enhanced expressions of early-stage osteogenic markers (RUNX2 and alkaline phosphatase) for cells undergoing osteogenic differentiation with the osteogenic medium on MeHA–SiO₂ hydrogel, compared to those cultured on MeHA hydrogel. Importantly, the cells cultivated on MeHA–SiO₂ expressed a ~5-fold increase in nuclear localization ratio of the yes-associated protein, which is known to be mechanosensory in stem cells, compared to the cells cultured on MeHA hydrogel, thereby promoting osteogenic differentiation of stem cells. These findings demonstrate the potential use of nanomaterials into a soft polymeric matrix for enhanced cell adhesion and provide valuable guidance for the rational design of biomaterials for implantation.

Keywords: cell adhesion; nanocomposite hydrogel; stem cell differentiation; mechanotransduction



Citation: Yin, B.; Yang, H.; Yang, M. Integrating Soft Hydrogel with Nanostructures Reinforces Stem Cell Adhesion and Differentiation. *J. Compos. Sci.* **2022**, *6*, 19. <https://doi.org/10.3390/jcs6010019>

Academic Editor:
Francesco Tornabene

Received: 8 December 2021

Accepted: 4 January 2022

Published: 6 January 2022

Publisher's Note: MDPI stays neutral with regard to jurisdictional claims in published maps and institutional affiliations.



Copyright: © 2022 by the authors. Licensee MDPI, Basel, Switzerland. This article is an open access article distributed under the terms and conditions of the Creative Commons Attribution (CC BY) license (<https://creativecommons.org/licenses/by/4.0/>).

1. Introduction

The growth and functions of mammalian cells, including stem cells, are highly associated with biophysical cues, such as matrix stiffness of the surrounding extracellular matrix (ECM) [1]. This microenvironment is known as a “stem cell niche” that contains biochemical and biophysical attributes of ECM to govern stem cell self-renewal and differentiation [2]. Mesenchymal stem cells (MSCs) are a promising source of regenerative medicine for tissue engineering and regenerative therapeutics. Biophysical cues, such as matrix stiffness [3,4], surface topography [5–7], ligand spacing [8,9], and ligand dynamics [10–13], are shown to regulate cellular behaviors and cell fates. In particular, MSCs can sense and respond to matrix stiffness, which is indicated by Young’s modulus and represents the elasticity of the matrix [2]. For instance, MSCs preferentially differentiate into neural cells or osteoblasts on soft or stiff matrices, respectively [14]. Thus, engineering biomimetic polymers with controlled stiffness, such as hydrogels, provide a biocompatible platform to facilitate the study of cell-matrix interaction and potentially optimize the differentiation outcomes for stem cell therapy [15].

Integrin is the well-known transmembrane protein that transduces the biophysical information into intracellular biochemical signals (outside-in) [16]. It is specific to ECM-derived bioactive peptide (e.g., Arg-Gly-Asp/RGD) forming the integrin-ECM bond (molecular clutches) and mediates the formation of focal adhesions (FAs) that can respond to mechanical force loading (inside-out) [17]. Further recruitment of the integrin-ECM bond by lateral clustering enhances the maturation of FA, which induces mechanosensing signaling and influences MSC differentiation [18]. Literature shows that a stiff or rigid matrix fosters this maturation by providing stable anchorage points and enabling cellular mechanical feedback to the matrix [3]. However, high stiffness hydrogels are often fabricated by high solid-to-content polymers, or a high degree of crosslinking that may increase the difficulty and time of enzymatic degradation and impose local toxicity or immune response to cells [1,19]. Thus, a soft or low concentration-made hydrogel is potentially more favourable for cell culture and *in vivo* implantation in the field of tissue engineering.

Surface modulation of biomaterials with the presentation of cell adhesive ligand is essential for integrin clustering and subsequent cell spreading. The mechanical property of the biomaterial surface can directly attribute to the strength of anchorage between integrins and ligands. However, matrix softness may destabilize this engagement and lead to the disruption of successive FA formation. To utilize soft hydrogel as the cytocompatible biomaterial for tissue engineering, it is highly desirable to modulate the hydrogel surface that can facilitate FA formation and subsequent mechanosensing of the cultured stem cells, especially by employing nanostructure integration.

Herein, we report a cytocompatible soft nanocomposite hydrogel substrate composed of natural biopolymer, methacrylated hyaluronic acid (MeHA) hydrogel conjugated with RGD-bearing silica nanoparticles (SiO_2 NPs, forming MeHA- SiO_2), to regulate the cell adhesion behaviour and differentiation of human MSCs (hMSCs, Figure 1a). SiO_2 NPs are a well-known biocompatible nanomaterial and provide a facile surface functionalization property [20]. We postulate that hMSCs are unable to develop mature FA on soft MeHA hydrogel, while MeHA- SiO_2 hydrogel of similar stiffness and ligand density to the MeHA hydrogel provides localized RGD-integrin clustering points to strengthen hMSCs adhesion on such soft polymeric matrices (Figure 1b). Our results show that hMSCs attach well with mature FA formation on soft MeHA- SiO_2 hydrogel (2.79 ± 0.31 kPa) but fail to adhere or spread well on MeHA soft hydrogel (3.08 ± 0.68 kPa). We reveal that FA maturation in hMSCs enhances their mechanosensing signalling, contributing to promoted osteogenic differentiation in the MeHA- SiO_2 group. We believe that our platform provides a promising design to encourage the application of soft nanocomposite materials in tissue engineering.

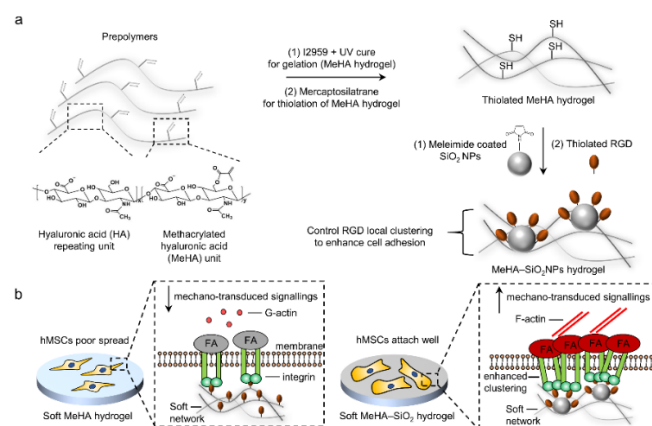


Figure 1. Schematic illustration of integrating nanostructures into soft hyaluronic acid (HA) hydrogel for enhancing human mesenchymal stem cell (hMSC) adhesion. (a) Synthetic routes of methacrylated HA (MeHA) hydrogel with cell-adhesive ligands (RGD)-bearing silica nanoparticles (SiO_2 NPs) conjugation, forming nanocomposite hydrogel (MeHA- SiO_2). (b) proposed mechanisms of differential cell behaviours on bare soft MeHA hydrogel (left) and soft MeHA- SiO_2 hydrogel (right), respectively.

2. Materials and Methods

2.1. Fabrication of Methacrylated Hyaluronic Acid and MeHA Hydrogel

MeHA with a methacrylation degree at ~30% was synthesized from sodium hyaluronate with a molecular weight of 40–70 k Da (Lifecore, Beijing, China) according to the previous report [15]. To conjugate RGD peptide to MeHA polymer, 7.2 mg of GCGYGRGDSPG (GenScript, Beijing, China) was added to 100 mg MeHA in 10 mL phosphate buffer at pH 8.0 with the presence of 5 mM tris(2-carboxyethyl) phosphine hydrochloride for 24 h under a dark condition (Figure S1), followed by dialysis of the products against 100 mM sodium chloride for 2 days and then deionized (DI) water for another 2 days. Subsequently, the solution was collected for freezing and undergoing lyophilization (freeze-drying). This RGD conjugation consumed ~3% of the methacrylate groups in MeHA polymers. Before gelation, 1% *w/v* MeHA precursor solution (with or without RGD peptide conjugation) was mixed with 0.05% *w/v* photo-initiator (2-methyl-1-[4-(hydroxyethoxy) phenyl]-2-methyl-1-propanone (I2959, J&K Chemicals Ltd., Shanghai, China) in phosphate buffer saline (PBS, Thermofisher, Shanghai, China) at pH 7.4. The precursor mixture was injected onto a 24-well culture plate lid circular well space (Corning, Wujiang, China) as the mold, and the well was then covered with a thiolated glass coverslip for the immobilization of hydrogel onto the glass. The precursor solution was exposed to ultraviolet (UV) light at 365 nm (7 mW/cm²) for 30 min. The size of the resultant hydrogel was 1.8 cm in diameter (circular shape) and ~200 µm in thickness. The UV-induced as-prepared MeHA hydrogel was washed with PBS for 3 times for further applications.

2.2. Synthesis and Functionalization of Silica Nanoparticles

Silica nanoparticles (SiO₂ NPs) were prepared according to the previous report [21]. Briefly, a modified Stober process was performed by the following reactant molar ratio: [1 tetraethyl orthosilicate (TEOS, J&K Chemicals Ltd., Shanghai, China): 0.02 L-lysine (J&K Chemicals Ltd., Shanghai, China): 162 H₂O] with stirring for 12 h at 60 °C. Subsequently, 0.4 mol of TEOS was added to the reaction mixture at the same condition for another 24 h. For synthesizing fluorescein 5-isothiocyanate (FITC)-labelled-SiO₂ NPs, 1 mg/mL of FITC was loaded into the solution simultaneously with the addition of TEOS. The resulting NPs were washed with DI water for 3 times and stored in DI water. Next, 25 mg/mL of the as-prepared SiO₂ NPs were amino-functionalized by mixing with 200 µL of (3-Aminopropyl)triethoxysilane (APTES, Alrich Sigma, Shanghai, China) in 50 mL ethanol and stirring for overnight. The amino-functionalized SiO₂ NPs (25 mg/mL) were further conjugated with a short linker (4-maleimidobutyric acid N-hydroxysuccinimide ester, Mal-NHS, Aladdin) at 100 µg/mL in PBS at pH 7.4 with stirring overnight. The NPs were washed with PBS for 3 times and stored at 4 °C temporarily until further use.

2.3. Immobilized of RGD-Bearing SiO₂ NPs onto MeHA Hydrogel (MeHA–SiO₂)

The as-prepared MeHA hydrogel without RGD conjugation was thiolated using mercaptosilatrane, according to the previous report [11]. The maleimide-functionalized SiO₂ NPs (from 0 to 100 µg/mL) were conjugated onto the thiolated MeHA hydrogel in PBS at pH 7.4 for overnight. The hydrogel was further washed by PBS for three times (15 min for each washing). The saturated concentration was determined at 25 µg/mL by scanning electron microscopy (SEM). Subsequently, the thiolated RGD peptides (100 µg/mL) were conjugated onto the immobilized SiO₂ NPs surface. Non-bioactive peptides RAD (100 µg/mL) were used to replace RGD as the control group.

2.4. Quantification of Conjugated RGD Number in the Hydrogel

Ellman's reagent (Thermofisher Scientific, Shanghai, China) was used to quantify the reacted RGD peptides according to the manufacturer's instructions. Briefly, 20 µL of the remaining supernatant collected from Sections 2.1 or 2.3 (after RGD conjugation) was mixed with 50 µL of Ellman's reagent and 100 µL assay buffer for 15 min at room temperature with gentle shaking. Subsequently, the absorbance of the resultant solution was measured at

412 nm. In parallel, a standard curve of absorbance vs. known RGD peptide concentration was measured for calculated the sample. 1 thiol group was assumed to be equivalent to 1 RGD peptide. Three independent samples were collected for quantification.

2.5. Material Characterizations

Transmission electron microscopy (TEM operative at 120 kV, Hitachi, Tokyo, Japan), scanning electron microscopy (SEM, JOEL, Tokyo, Japan) with energy dispersive X-ray spectrum (EDS) characterization, and dynamic light scattering (DLS, Malvern Kinexus, Cambridge, United Kingdom) were employed to measure the morphology (TEM and SEM) and size distribution (TEM and DLS) of the as-prepared nanomaterials. Fourier-transform infrared spectroscopy (FTIR, Thermo Nicolet, Shanghai, China) characterized the new bonding for each conjugation. ^1H nuclear magnetic resonance (NMR, Bruker, Karlsruhe, Germany) was used to characterize the methacrylation degree of MeHA. Rheometer (Malvern Kinexus, Cambridge, United Kingdom) was used to measure the mechanical stiffness of the as-prepared hydrogel.

2.6. Cell Culture

hMSCs were purchased from Lonza (Bioscience), and the cells were passaged up to the fourth generation (P4) in a 10 mm plastic culture dish (treated, Corning, Wujiang, China). The hydrogel was fabricated in biological safety cabinet and sterilized by UV exposure for at least 1 h before the cell culture. Subsequently, the cells were trypsinized and cultured onto the hydrogel at 5000 cells/cm² at 37 °C and 5% CO₂. The basal culture medium was composed of α -minimum essential medium, 10% fetal bovine serum, 1% streptomycin/penicillin, and 1% L-glutamine (ThermoFisher Scientific). A total of 10 ng/mL of FGF2 protein (Sinobiological, Beijing, China) was used as the growth factor during the culture. For induced osteogenic differentiation, FGF2 was removed, and the basal culture medium was supplemented with 100 nM dexamethasone (Sigma, Shanghai, China), 1 μM indomethacin (J&K Chemicals Ltd., Shanghai, China), 10 mM BPG, and L-ascorbic acid 2-phosphate (Sigma, Shanghai, China). The differentiation was induced for 7 days after 1-day of initial cell adhesion (at 5000 cells/cm²) in basal culture medium at 37 °C and 5% CO₂. All cell culture and differentiation studies were performed in 24-well culture plates (Corning, Wujiang, China) with 1 mL basal culture or induced differentiation medium. The culture medium was refreshed every 2 days. The group that cells were cultured on a glass substrate (1.8 cm \times 1.8 cm) was used as a positive control. The group in which cells were cultured on MeHA hydrogel conjugated with RAD peptides was used as a negative control. The hydrogel incubated with the culture medium only was considered as a blank control.

2.7. Histochemistry Staining & Fluorescent Imaging

After the cells were cultured for 1 day (cell adhesion assay) or 7 days (cell differentiation assay), the culture medium was removed, and the cells were washed with PBS at pH 7.4 for three times, followed by cell fixation by 4% paraformaldehyde (J&K Chemicals, Ltd., Shanghai, China) for 30 min at room temperature; the permeability of cell membranes was increased by treating with 0.02% Triton-X100 (Sigma Aldrich, Inc., Shanghai, China). The following reagents were used for the histochemistry staining: 1:500 Rhodamine-phalloidin (Cytoskeleton, Inc., Hong Kong) for visualizing F-actin; 1:400 anti-RUNX2 (mouse monoclonal IgG, Santa Cruz Biotechnology, Inc., Dallas, TX, USA) for staining RUNX2; 1:400 anti-vinculin (mouse monoclonal IgG, Sigma Aldrich, Inc.); 1:400 anti-YAP (mouse monoclonal IgG, Santa Cruz Biotechnology, Inc.); cell nuclei were stained with 4-6-Diamidino-2-phenylin (DAPI 1:2000; Molecular Probes, Inc.). Goat anti-mouse IgG secondary antibodies with Alexa Fluor 488 in 1:1000 (Santa Cruz Biotechnology, Inc., Dallas, TX, USA) was used for the counter fluorescent labelling. Live-dead staining was performed by using calcein-AM (~5 μM , Molecular Probes, Inc., Eugene, OR, USA) and propidium iodide to show the cell viability (0.5 μM , Molecular Probes, Inc., Eugene, OR, USA). For alkaline phosphatase (ALP) staining, 4% *v/v* naphthol AS-XX phosphate (Sigma Aldrich,

Inc.) in fast blue RR salt solution (Sigma Aldrich, Inc.) was used to stain the cell samples for 45 at 37 °C in the dark. The stained cells were imaged under a Nikon Eclipse confocal microscope. The excitation/emission pair for rhodamine (F-actin staining), Alexa Fluor 488, and DAPI were 556/573, 495/518, and 405/470 nm, respectively. The photography conditions such as exposure time, signal gain, and laser intensity were controlled the same for each group.

2.8. Image and Statistical Analysis

All images (material characterizations and cell images) were analyzed using Image J (NIH). Mnova (Mestrelab, Compostela, Spain) was used to analyze and export the NMR data. DelsaMax (Beckman Coulter, Shanghai, China) was used to analyze and export DLS data. Cell adherent percentage, spreading, and YAP and RUNX2 nuclear localization ratios were measured according to the previous report [22,23]. Initial cell adherent percentage was quantified by measuring the percentage of the attached cell number divided by seeding cell number from three independent gels for each group after 1 day of culture. For cell spreading evaluation, Image J was used to measure the area of interest along the F-actin boundary of at least 30 cells from three independent gels for each group were analyzed. Nuclear localization ratio quantification of YAP or RUNX2 was calculated by the ratio of the nuclear fluorescent intensity over the cytoplasmic fluorescent intensity of at least 50 cells from three independent gels for each group. The percentage of ALP positively stained cells was quantified by counting the number of ALP-stained cells over the overall cell number from three independent gels for each group. Analysis of co-variance (one-way ANOVA) was performed on all the statistics.

3. Results and Discussion

3.1. Characterization of the Soft Nanocomposite Hydrogel

We methacrylated HA polymers (40–70 kDa) with ~30% methacrylation degree as the hydrogel precursor (Figure S2). The gelation of MeHA hydrogel was induced by UV light with the presence of photo-initiators, and the hydrogel network was observed under SEM (Figure 2a). The mechanical stiffness of the as-prepared hydrogel was 3.08 ± 0.68 kPa (Figure 2e), considered as the soft matrix range [24]. This soft polymeric matrix provides a scaffold for the immobilization of SiO₂ NPs. Subsequently, we fabricated SiO₂ NPs with a diameter of 31.4 ± 2.5 nm (Figures 2b and S3) and conjugated the NPs onto the as-prepared MeHA hydrogel, forming the nanocomposite hydrogel (MeHA–SiO₂). The NPs stably attached to the hydrogel network, confirmed by SEM imaging (Figure 2a). In addition, FTIR spectra indicated the successful conjugation of SiO₂ NPs to MeHA hydrogel with the peak at 1066–1150 cm⁻¹, responsible for siloxane vibrations and the subsequent RGD peptide conjugation onto the SiO₂ NPs with the peak at 1275 cm⁻¹, responsible for amide II N–H deformation (Figure 2c). The surface density of the immobilized SiO₂ NPs was strictly controlled to be 134 ± 12 particles/μm² for each gel. More importantly, we illustrated that the stiffness of MeHA–SiO₂ hydrogel (2.79 ± 0.31 kPa) was similar to that of MeHA hydrogel (Figure 2e), indicating that the integration of SiO₂ NPs to the synthesized hydrogel network did not strengthen its mechanical stiffness. Moreover, we confirmed that the number of immobilized RGD peptides was maintained similarly in these two gels (Figure 2d). We observed that the pore size of the MeHA hydrogel was >100 nm, large enough for the infiltration of SiO₂ NPs (size = 31.4 ± 2.5 nm) into the hydrogel network for the coating during the fabrication. Our magnified SEM image indicates that the inner structure of MeHA–SiO₂ hydrogel contains SiO₂ NPs (Figure S4a), as evidenced by the EDS characterization (Figure S4b). Thus, we believe that the RGD peptide conjugation is not restricted to the surface of MeHA–SiO₂ hydrogel, but rather the entire network, because of its thin layer and large pore size. We also labelled the immobilized SiO₂ with FITC and performed fluorescent scanning along the z-axis of the hydrogel with cell culture. Our data show that the hydrogel layer contained an enriched FITC fluorescent signal (Figure S4c), suggesting that SiO₂ NPs were embedded throughout the hydrogel network. Thus, we

believe that the RGD peptides were also uniformly coupled in the whole MeHA–SiO₂ hydrogel, similar to that in MeHA hydrogel. In short, we successfully synthesized a soft nanocomposite hydrogel that can potentially manipulate the integrin-ligand complex to support cell adhesion on the soft matrix.

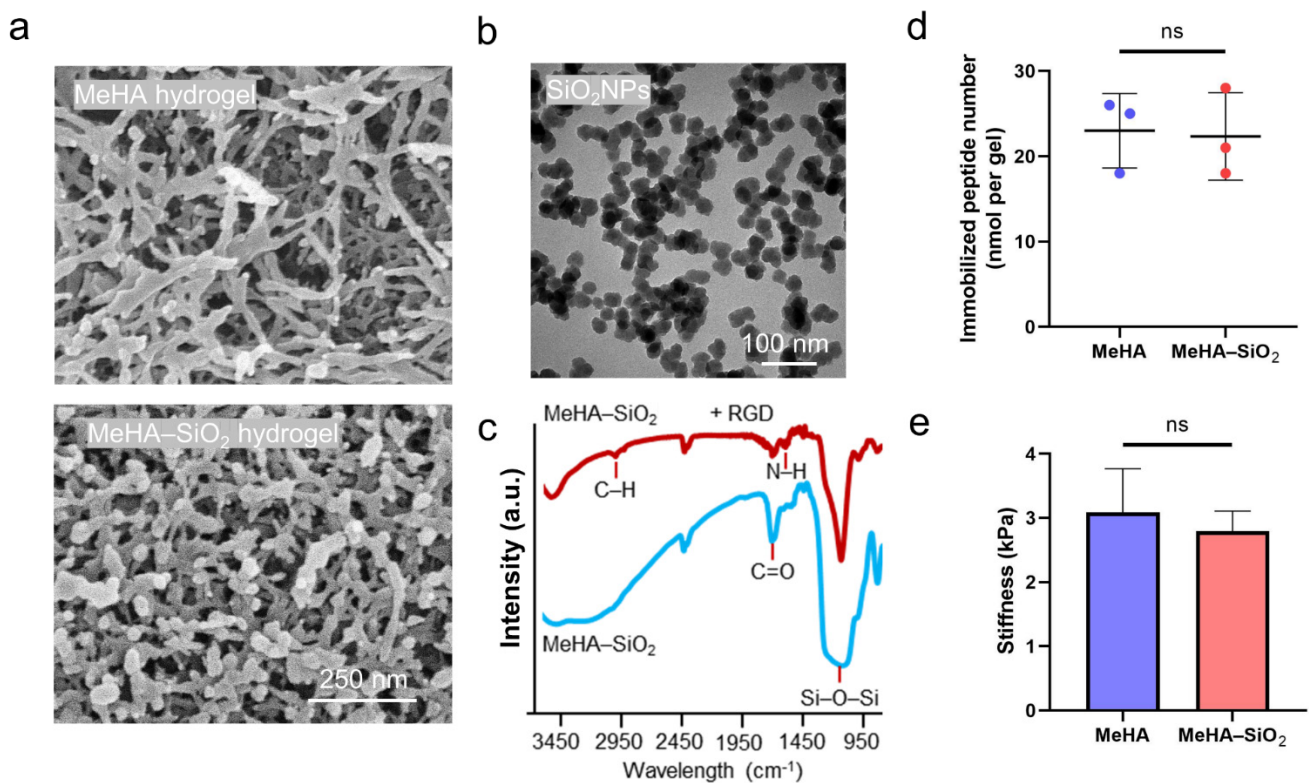


Figure 2. Material characterization of the soft nanocomposite hydrogel. (a) scanning electron microscopic (SEM) images of MeHA (up) and MeHA–SiO₂ (down) hydrogels. (b) Transmission electron microscopic (TEM) images of the prepared SiO₂ NPs. (c) Fourier-transformed infrared spectra of MeHA–SiO₂ hydrogel (blue line) and MeHA–SiO₂ hydrogel with RGD conjugation (red line). (d) quantification of immobilized RGD number in both hydrogels. (e) Stiffness measurement of the hydrogels. The error bars represent the s.e.m. ns represents statistically not significant by one-way ANOVA.

3.2. Enhanced Mechanosensing of hMSCs on the Soft Nanocomposite Hydrogel

To study how the local clustering of RGD peptides regulates cell adhesion, we cultured hMSCs onto MeHA and MeHA–SiO₂ hydrogels, respectively, for 24 h. Strikingly, we observed that hMSCs exhibited a higher percentage of initial cell attachment and cell spreading area on MeHA–SiO₂ than those on MeHA hydrogel (Figure 3a–c). Particularly, cells cultured on MeHA–SiO₂ hydrogel spread with polygonal shape while remaining spindle shape on MeHA hydrogel (Figure 3a), indicating a differential cell adhesive property between these two gels [25]. In contrast, replacing the immobilized RGD peptides with non-bioactive RAD resulted in minimal cell adhesion on both gels (Figure 3a–c). These control groups show that immobilized RGD peptide is necessary to mediate hMSC attachment to the MeHA hydrogel, and SiO₂ NPs passivated with RAD remain non-bioactive to influence cell adhesive behaviours. On the other hand, cells cultured on a glass substrate showed a high cell spreading area (Figure S5), consistent with the stem cell behaviour that cells attached well to a rigid substrate [6]. Thus far, these findings suggest that the immobilized SiO₂ NPs spatially manipulate RGD localization on their surface to control cell adhesion but the SiO₂ NPs without RGD do not intrinsically affect biological functions.

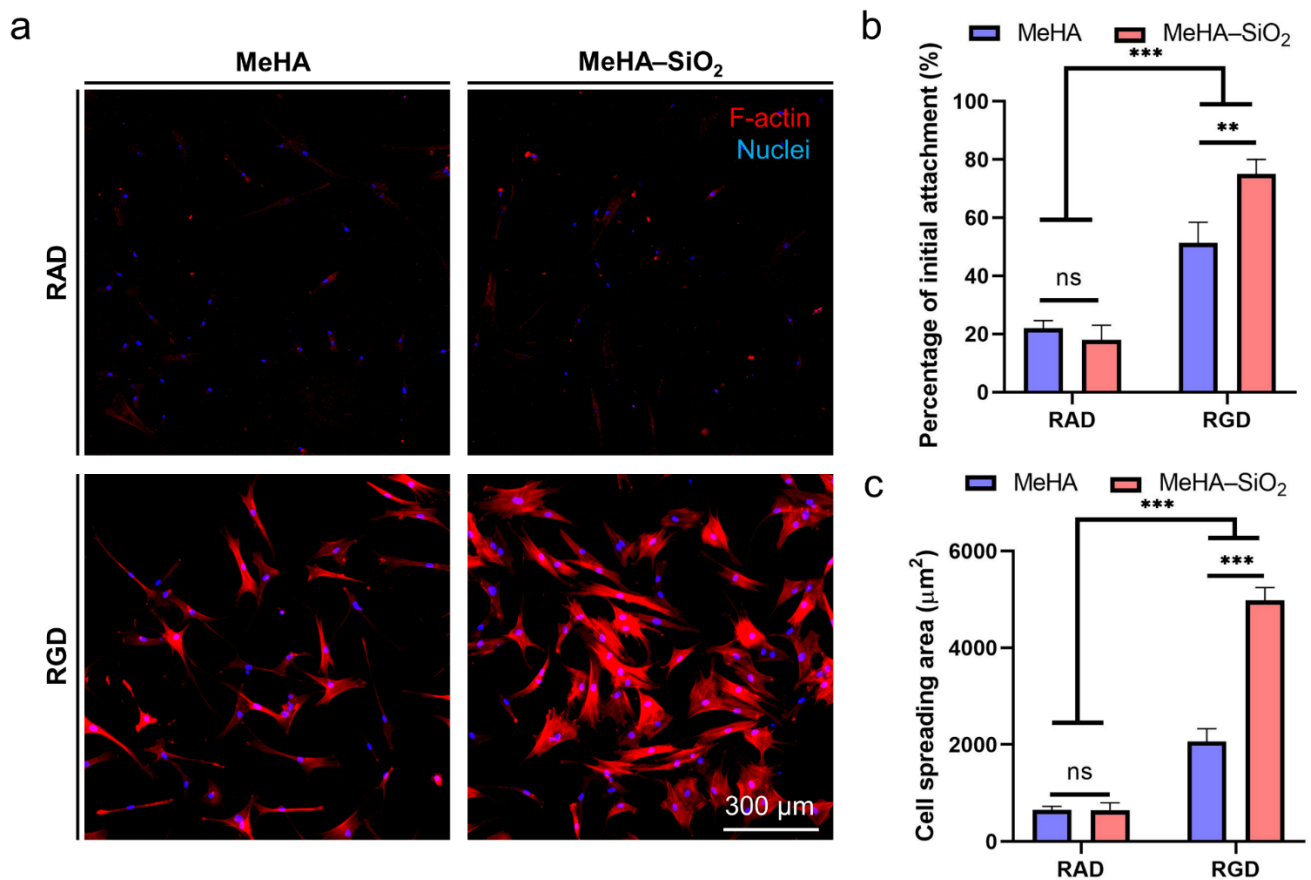


Figure 3. Microscopic observation of hMSC adhesive behaviours on soft nanocomposite hydrogel. (a) Cytoskeletal staining (F-actin, red) with nuclei (blue) staining of cells cultured on MeHA and MeHA-SiO₂ hydrogels for 24 h. RAD replaces RGD as a control group. Statistical quantification of (b) the percentage of initial cell attachment (24 h) and (c) cell spreading area. The error bars represent the s.e.m. ns represents statistically not significant and significance difference *p*-value: ** *p* < 0.001; *** *p* < 0.001 (one-way ANOVA).

Next, we examined whether the enhanced cell adhesion is mediated through the mechanotransduced signalling on MeHA-SiO₂ hydrogel. Vinculin is one of the main proteins recruited in FA complex [26]. Also, the maturation of FA formation is related to the strength of adhesion at the integrin-ligand complex [27]. Our results showed that hMSCs developed pronounced actin stress fibers and punctate vinculin staining at the site of FA on MeHA-SiO₂ hydrogel to support cell adhesion and mechanotransduction (Figure 4a). However, these developments were much less evident in hMSCs grown on MeHA hydrogel. The size of vinculin punctate in the MeHA-SiO₂ group was ~3-fold larger than those in the MeHA group (Figure 4b), suggesting that MeHA-SiO₂ favoured the maturation of FA and cell spreading, which were hindered by soft MeHA hydrogel alone. The assembly of the stress fibers, F-actin constructs the cytoskeleton to support cellular locomotion and increases cytoskeletal tension [28]. This tension enhancement is shown to activate the signalling pathway of yes-associated protein (YAP), a mechanosensitive transcriptional factor that is localized in the nucleus by the mechanical force transmission to regulate stem cell differentiation, such as osteogenic differentiation of hMSCs [29]. Thus, we examined the spatial distribution of YAP in hMSCs cultured on both gels. Significantly, the immunostaining results revealed that intense YAP localized at nuclei in hMSCs cultured on MeHA-SiO₂ hydrogel (Figure 4a). In contrast, YAP was evenly distributed throughout the cytosol in cells grown on MeHA hydrogel, with a ~5-fold less YAP nuclear localization ratio than those in the MeHA-SiO₂ group (0.59 ± 0.22 vs. 3.20 ± 0.79). It is known that the formation and maturation of FAs require active actomyosin-mediated mechanical feedback

between the extracellular environment and the intracellular cytoskeletal structures upon the initial ligation of the integrin receptor and its ligands presented on the matrix [14]. Moreover, the focal adhesion assembly is one of the key factors to regulate YAP translocation to the nucleus for gene transcription regulation [18]. Importantly, cells failed to adhere and spread well on the hydrogels with RAD conjugation, suggesting that RGD peptide is the crucial factor to mediate cell adhesion and associate mechanosensing. In addition, MeHA–SiO₂ hydrogel significantly improved FA maturation, reflected by the pronounced size of FA measured by the immunostaining compared to MeHA hydrogel. These results support our hypothesis that the fabricated soft nanocomposite hydrogel strengthens FA formation and mediate mechanosensing.

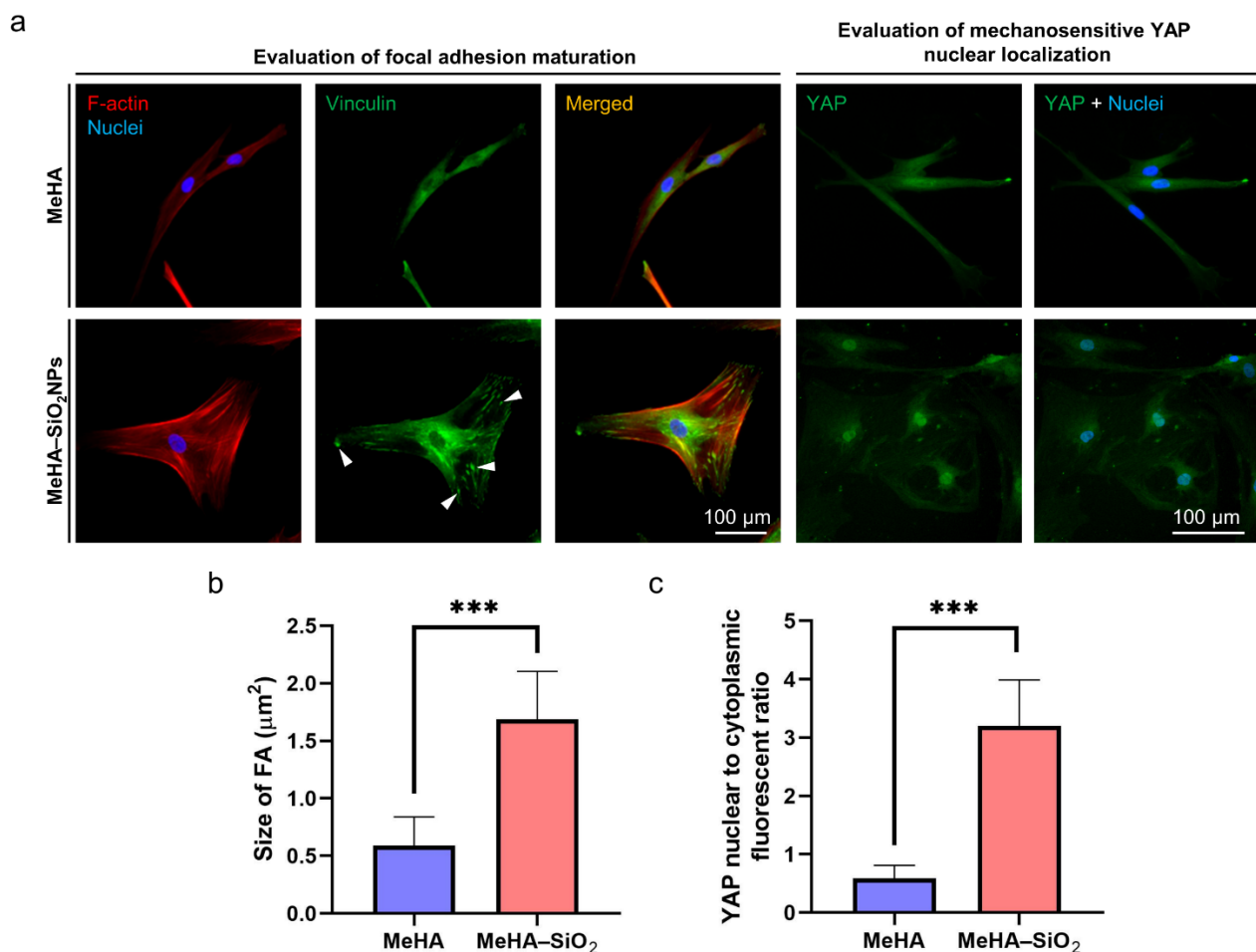


Figure 4. Evaluation of mechanotransduced events of hMSCs cultured on the soft nanocomposite hydrogel. (a) Immunofluorescent staining of focal adhesion (FA) marker, vinculin (green at the left panel) and mechanosensitive marker, yes-associated protein (YAP, green at the right panel) of cells cultured on the hydrogels for 24 h. The error bars represent the s.e.m. Statistical analysis of (b) size of FA and (c) YAP nuclear localization ratio. Significance difference p -value: *** $p < 0.001$ (one-way ANOVA).

3.3. Local RGD Clustering Supports Stem Cell Osteogenic Differentiation on Soft Matrix

After culturing cells in basal medium on the hydrogels for 1 day, we refreshed the medium with an inductive medium to induce hMSCs into osteogenic differentiation for 7 days to examine whether the soft nanocomposite hydrogel could impact stem cell differentiation. We investigated the expression of ALP and RUNX2 as the two typical early-stage markers of stem cell osteogenic differentiation [30]. Strikingly, we observed that the MeHA–SiO₂ group showed more intense staining and positively stained cells against ALP than the MeHA group (Figure 5a). In addition, hMSCs expressed highly localized RUNX2 at

their nuclei on MeHA–SiO₂ hydrogel but weakly transferred RUNX2 to the nucleus on MeHA hydrogel as shown by the immunostaining results (Figure 5a–c). In contrast, hMSCs without osteogenic medium showed significantly low levels of ALP and RUNX2 on MeHA hydrogel, indicating that undifferentiated hMSCs expressed very low basal expression levels of these two markers (Figure S6). These results are consistent with the previous findings that the activation of the mechanotransduction pathway (YAP) is positively associated with the osteogenic differentiation of stem cells [31,32]. More importantly, our findings illustrate that the implementation of the nanostructure re-arranges the spatial distribution of cell-adhesive peptides to reinforce stem cell adhesion and differentiation on soft matrix.

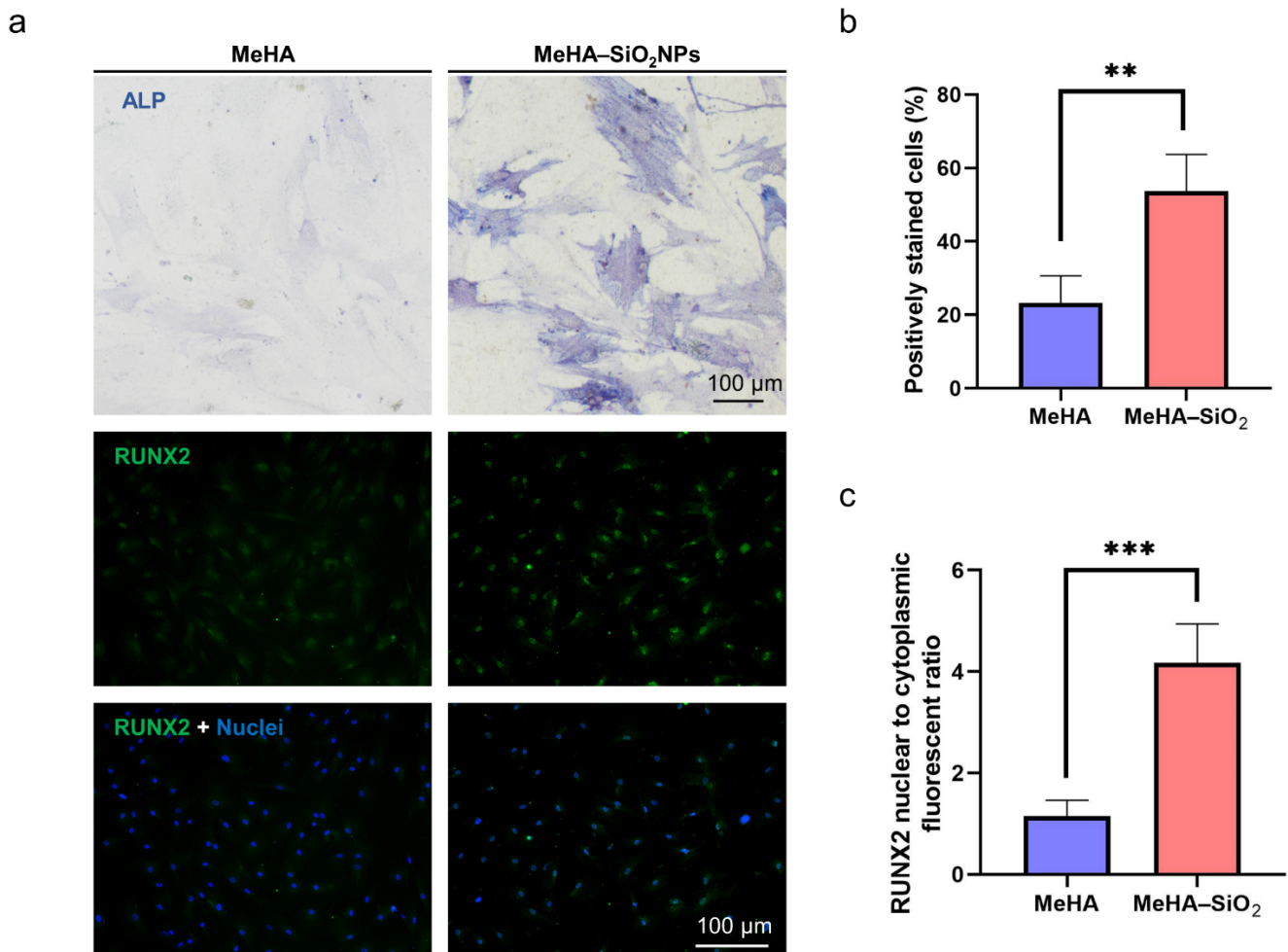


Figure 5. Evaluation of the effect on stem cell differentiation by the soft nanocomposite hydrogel. (a) Staining of osteogenic differentiation markers, alkaline phosphatase (ALP) and RUNX2 at the early stage after hMSCs cultured on the hydrogels for 7 d. Statistical analysis of (b) the percentage of ALP positively stained cells and (c) RUNX2 nuclear localization ratio. The error bars represent the s.e.m. Significance difference *p*-value: ** *p* < 0.01, and *** *p* < 0.001 (one-way ANOVA).

4. Conclusions

In summary, this study demonstrates a soft nanocomposite hydrogel by simply integrating nanostructures into the hydrogel network to study the effect of RGD clusters on stem cell adhesion, spreading, and differentiation on soft matrix. Our results illustrate that the immobilization of SiO₂ NPs onto soft MeHA hydrogel localizes multiple strands of RGD peptides on their surface that enhances cell adhesion, spreading, and mechanosensing signalings and associated differentiation at the early stage, hardly achieved by soft MeHA hydrogel alone. These findings highlight the importance of anchoring nanomaterials in the

soft polymeric matrix in biomaterial design to regulate critical cellular responses and assist translational application of hydrogel implantation in tissue engineering.

Supplementary Materials: The following are available online at <https://www.mdpi.com/article/10.3390/jcs6010019/s1>, Figure S1: Synthetic route of RGD-coupled MeHA hydrogel. Figure S2: ¹H NMR spectrum of MeHA polymers, Figure S3: DLS data of as-prepared and functionalized SiO₂ NPs. Figure S4: Exploration of immobilized SiO₂ NPs in MeHA hydrogel network. Figure S5: Evaluation of cell spreading of cells cultured on a glass substrate. Figure S6: Examination of the expression level of ALP and RUNX2 in undifferentiated hMSCs.

Author Contributions: Conceptualization, B.Y. and M.Y.; methodology, H.Y.; software, B.Y.; validation, M.Y.; data curation, B.Y.; writing—original draft preparation, B.Y. and M.Y.; writing—review and editing, B.Y. and M.Y.; visualization, B.Y.; supervision, M.Y.; project administration, M.Y.; funding acquisition, M.Y. All authors have read and agreed to the published version of the manuscript.

Funding: National Natural Science Foundation of China (NSFC) (Grant Nos. 31771077), the Research Grants Council (RGC) of Hong Kong Collaborative Research Grant (C5110-20GF), the Research Grants Council (RGC) of Hong Kong General Research Grant (PolyU 15214619E and PolyU 15210818E), the Shenzhen-Hong Kong-Macao Science and Technology Plan Project (Category C, 202011033000095) the Hong Kong Polytechnic University Internal Fund (1-ZE1E).

Data Availability Statement: The data presented in this study are available on request from the corresponding author.

Acknowledgments: This work was supported by the University Research Facility in Life Sciences of PolyU.

Conflicts of Interest: The authors declare no conflict of interest.

References

1. Zhang, M.; Sun, Q.; Liu, Y.; Chu, Z.; Yu, L.; Hou, Y.; Kang, H.; Wei, Q.; Zhao, W.; Spatz, J.P.; et al. Controllable ligand spacing stimulates cellular mechanotransduction and promotes stem cell osteogenic differentiation on soft hydrogels. *Biomaterials* **2021**, *268*, 120543. [CrossRef]
2. Jhala, D.; Vasita, R. A Review on Extracellular Matrix Mimicking Strategies for an Artificial Stem Cell Niche. *Polym. Rev.* **2015**, *55*, 561–595. [CrossRef]
3. Ye, K.; Wang, X.; Cao, L.; Li, S.; Li, Z.; Yu, L.; Ding, J. Matrix Stiffness and Nanoscale Spatial Organization of Cell-Adhesive Ligands Direct Stem Cell Fate. *Nano Lett.* **2015**, *15*, 4720–4729. [CrossRef] [PubMed]
4. Yan, T.; Rao, D.; Chen, Y.; Wang, Y.; Zhang, Q.; Wu, S. Magnetic nanocomposite hydrogel with tunable stiffness for probing cellular responses to matrix stiffening. *Acta Biomater.* **2021**, *138*, 112–123. [CrossRef] [PubMed]
5. Hou, Y.; Yu, L.; Xie, W.; Camacho, L.C.; Zhang, M.; Chu, Z.; Wei, Q.; Haag, R. Surface Roughness and Substrate Stiffness Synergize To Drive Cellular Mechanoreponse. *Nano Lett.* **2020**, *20*, 748–757. [CrossRef]
6. Li, X.; Klausen, L.H.; Zhang, W.; Jahed, Z.; Tsai, C.T.; Li, T.L.; Cui, B. Nanoscale Surface Topography Reduces Focal Adhesions and Cell Stiffness by Enhancing Integrin Endocytosis. *Nano Lett.* **2021**, *21*, 8518–8526. [CrossRef]
7. Yin, B.; Ho, L.W.C.; Liu, S.; Hong, H.; Tian, X.Y.; Li, H.; Choi, C.H.J. Sub-10 nm Substrate Roughness Promotes the Cellular Uptake of Nanoparticles by Upregulating Endocytosis-Related Genes. *Nano Lett.* **2021**, *21*, 1839–1847. [CrossRef]
8. Wang, X.; Yan, C.; Ye, K.; He, Y.; Li, Z.; Ding, J. Effect of RGD nanospacing on differentiation of stem cells. *Biomaterials* **2013**, *34*, 2865–2874. [CrossRef]
9. Zheng, S.; Liu, Q.; He, J.; Wang, X.; Ye, K.; Wang, X.; Yan, C.; Liu, P.; Ding, J. Critical adhesion areas of cells on micro-nanopatterns. *Nano Res.* **2022**, *15*, 1623–1635. [CrossRef]
10. Zhang, J.; Wong, S.H.D.; Wu, X.; Lei, H.; Qin, M.; Shi, P.; Wang, W.; Bian, L.; Cao, Y. Engineering Photoresponsive Ligand Tethers for Mechanical Regulation of Stem Cells. *Adv. Mater.* **2021**, *33*, e2105765. [CrossRef]
11. Wong, S.H.D.; Wong, W.K.R.; Lai, C.H.N.; Oh, J.; Li, Z.; Chen, X.Y.; Yuan, W.H.; Bian, L.M. Soft Polymeric Matrix as a Macroscopic Cage for Magnetically Modulating Reversible Nanoscale Ligand Presentation. *Nano Lett.* **2020**, *20*, 3207–3216. [CrossRef] [PubMed]
12. Chen, X.; Lai, N.C.; Wei, K.; Li, R.; Cui, M.; Yang, B.; Wong, S.H.D.; Deng, Y.; Li, J.; Shuai, X.; et al. Biomimetic Presentation of Cryptic Ligands via Single-Chain Nanogels for Synergistic Regulation of Stem Cells. *ACS Nano* **2020**, *14*, 4027–4035. [CrossRef] [PubMed]
13. Wong, S.H.D.; Yin, B.H.; Yang, B.G.; Lin, S.E.; Li, R.; Feng, Q.; Yang, H.R.; Zhang, L.; Yang, Z.M.; Li, G.; et al. Anisotropic Nanoscale Presentation of Cell Adhesion Ligand Enhances the Recruitment of Diverse Integrins in Adhesion Structures and Mechanosensing-Dependent Differentiation of Stem Cells. *Adv. Funct. Mater.* **2019**, *29*, 1806822. [CrossRef]

14. Engler, A.J.; Sen, S.; Sweeney, H.L.; Discher, D.E. Matrix elasticity directs stem cell lineage specification. *Cell* **2006**, *126*, 677–689. [[CrossRef](#)]
15. Yang, B.; Wei, K.; Loebel, C.; Zhang, K.; Feng, Q.; Li, R.; Wong, S.H.D.; Xu, X.; Lau, C.; Chen, X.; et al. Enhanced mechanosensing of cells in synthetic 3D matrix with controlled biophysical dynamics. *Nat. Commun.* **2021**, *12*, 3514. [[CrossRef](#)]
16. Humphries, J.D.; Byron, A.; Humphries, M.J. Integrin ligands at a glance. *J. Cell Sci.* **2006**, *119*, 3901–3903. [[CrossRef](#)]
17. Desai, R.A.; Khan, M.K.; Gopal, S.B.; Chen, C.S. Subcellular spatial segregation of integrin subtypes by patterned multicomponent surfaces. *Integr. Biol.* **2011**, *3*, 560–567. [[CrossRef](#)] [[PubMed](#)]
18. Wong, D.S.; Li, J.; Yan, X.; Wang, B.; Li, R.; Zhang, L.; Bian, L. Magnetically Tuning Tether Mobility of Integrin Ligand Regulates Adhesion, Spreading, and Differentiation of Stem Cells. *Nano Lett.* **2017**, *17*, 1685–1695. [[CrossRef](#)]
19. Kong, D.; Megone, W.; Nguyen, K.D.Q.; Di Cio, S.; Ramstedt, M.; Gautrot, J.E. Protein Nanosheet Mechanics Controls Cell Adhesion and Expansion on Low-Viscosity Liquids. *Nano Lett.* **2018**, *18*, 1946–1951. [[CrossRef](#)]
20. Zhou, X.; He, X.; Shi, K.; Yuan, L.; Yang, Y.; Liu, Q.; Ming, Y.; Yi, C.; Qian, Z. Injectable Thermosensitive Hydrogel Containing Erlotinib-Loaded Hollow Mesoporous Silica Nanoparticles as a Localized Drug Delivery System for NSCLC Therapy. *Adv. Sci.* **2020**, *7*, 2001442. [[CrossRef](#)]
21. Xia, L.J.; Yao, B.B.; Shi, Z.K.; Wang, W.P.; Kan, Z. Fundamental method for controlling monodisperse silica nanoparticles dimension assisted by lysine. *J. Sol-Gel Sci. Technol.* **2019**, *92*, 134–145. [[CrossRef](#)]
22. Wong, S.H.D.; Xu, X.; Chen, X.; Xin, Y.; Xu, L.; Lai, C.H.N.; Oh, J.; Wong, W.K.R.; Wang, X.; Han, S.; et al. Manipulation of the Nanoscale Presentation of Integrin Ligand Produces Cancer Cells with Enhanced Stemness and Robust Tumorigenicity. *Nano Lett.* **2021**, *21*, 3225–3236. [[CrossRef](#)] [[PubMed](#)]
23. Choi, C.K.K.; Xu, Y.J.; Wang, B.; Zhu, M.; Zhang, L.; Bian, L. Substrate coupling strength of integrin-binding ligands modulates adhesion, spreading, and differentiation of human mesenchymal stem cells. *Nano Lett.* **2015**, *15*, 6592–6600. [[CrossRef](#)] [[PubMed](#)]
24. Tong, X.; Jiang, J.; Zhu, D.; Yang, F. Hydrogels with Dual Gradients of Mechanical and Biochemical Cues for Deciphering Cell-Niche Interactions. *ACS Biomater. Sci. Eng.* **2016**, *2*, 845–852. [[CrossRef](#)] [[PubMed](#)]
25. Kang, H.; Jung, H.J.; Wong, D.S.H.; Kim, S.K.; Lin, S.; Chan, K.F.; Zhang, L.; Li, G.; Dravid, V.P.; Bian, L. Remote Control of Heterodimeric Magnetic Nanoswitch Regulates the Adhesion and Differentiation of Stem Cells. *J. Am. Chem. Soc.* **2018**, *140*, 5909–5913. [[CrossRef](#)]
26. Bays, J.L.; DeMali, K.A. Vinculin in cell-cell and cell-matrix adhesions. *Cell Mol. Life Sci.* **2017**, *74*, 2999–3009. [[CrossRef](#)]
27. Elineni, K.K.; Gallant, N.D. Regulation of cell adhesion strength by peripheral focal adhesion distribution. *Biophys. J.* **2011**, *101*, 2903–2911. [[CrossRef](#)]
28. Lehtimäki, J.I.; Rajakylä, E.K.; Tojkander, S.; Lappalainen, P. Generation of stress fibers through myosin-driven reorganization of the actin cortex. *eLife* **2021**, *10*, e60710. [[CrossRef](#)]
29. Driscoll, T.P.; Cosgrove, B.D.; Heo, S.J.; Shurden, Z.E.; Mauck, R.L. Cytoskeletal to Nuclear Strain Transfer Regulates YAP Signaling in Mesenchymal Stem Cells. *Biophys. J.* **2015**, *108*, 2783–2793. [[CrossRef](#)]
30. Li, R.; Li, J.; Xu, J.; Wong, D.S.H.; Chen, X.; Yuan, W.; Bian, L. Multiscale reconstruction of a synthetic biomimetic micro-niche for enhancing and monitoring the differentiation of stem cells. *Biomaterials* **2018**, *173*, 87–99. [[CrossRef](#)]
31. Hong, H.; Min, S.; Koo, S.; Lee, Y.; Yoon, J.; Jang, W.Y.; Kang, N.; Thangam, R.; Choi, H.; Jung, H.J.; et al. Dynamic Ligand Screening by Magnetic Nanoassembly Modulates Stem Cell Differentiation. *Adv. Mater.* **2021**, e2105460. [[CrossRef](#)] [[PubMed](#)]
32. Yuan, W.; Wang, H.; Fang, C.; Yang, Y.; Xia, X.; Yang, B.; Lin, Y.; Li, G.; Bian, L. Microscopic local stiffening in a supramolecular hydrogel network expedites stem cell mechanosensing in 3D and bone regeneration. *Mater. Horiz.* **2021**, *8*, 1722–1734. [[CrossRef](#)] [[PubMed](#)]